Monte Carlo optimization based QSAR modeling of the cytotoxicity of acrylic acid-based dental monomers

MIRJANA BOŠKOVIĆ[1], SAŠA STANKOVIĆ[1], JELENA V. ŽIVKOVIĆ[2]
and ALEKSANDAR M. VESELINOVIĆ[2]*

[1]Department for Prosthetic Dentistry, Faculty of Medicine, University of Niš, Bulevar Dr Zorana Đinđića 81, 18000 Niš, Serbia and [2]Departmant of Chemistry, Faculty of Medicine, University of Niš, Bulevar Dr Zorana Đinđića 81, 18000 Niš, Serbia

Abstract: Acrylic acid derivatives are extensively utilized as initial monomers in dental materials. Nevertheless, these substances exhibit cytotoxicity towards different cell types, a phenomenon that must be reduced in future materials. The primary objective of this research is to establish a QSAR model for the prediction of cytotoxic effects and to identify molecular fragments and descriptors with mechanistic interpretations that play a role in cytotoxic effects. The Monte Carlo optimization technique employed QSAR models that are not reliant on conformation. These models utilized both molecular graph-based and SMILES-based descriptors. By employing a variety of statistical methodologies, an assessment of the predictive capabilities and resilience of the established QSAR models was achieved. The demonstrated numerical values used for their validation underscore the strong suitability of these QSAR models. The Monte Carlo optimization technique effectively identified molecular fragments represented in QSAR modeling through the use of SMILES notation, elucidating their impact on cytotoxicity, both positively and negatively. Given that the majority of molecular databases adhere to this molecular structure conformation, the featured QSAR models can serve as a rapid and precise screening tool for novel dental monomers.

Keywords: QSAR; cytotoxicity; dental material; composite resin; SMILES; Monte Carlo optimization.

INTRODUCTION

Numerous dental procedures necessitate the utilization of polymers, which are composed of methacrylate-based monomers, including monomethacrylates or dimethacrylates.[1,2] Some of the most frequently employed monomers in this con-

---

BOŠKOVIĆ *et al.*

text include urethane dimethacrylate (UDMA), triethylene glycol dimethacrylate (TEGDMA), 2-hydroxyethyl methacrylate (HEMA), bisphenol-A glycidil dimethacrylate (Bis-GMA), as well as other more recent functionalized monomers.[1–3] The biocompatibility of these materials holds significant relevance for clinical applications, considering that oral tissues come into direct contact with them.[4] In dental practice, direct restorations involving dental adhesives and resin composites involve interaction with sensitive dentin-pulp complexes and acrylic acid-based monomers. This interaction can result in the diffusion of monomers from the restorative material through dentinal tubules, potentially causing adverse effects on pulp cells and compromising tooth vitality.[5,6] Literary sources indicate certain biological effects, such as the mutagenicity of various monomers and the genotoxicity and estrogenicity of Bis-GMA.[7] The primary mechanism underlying the free-radical polymerization reaction in dental materials is associated with methacrylate-based monomers. This chemical process may be linked to incomplete monomer conversion, resulting in the presence of unreacted monomers.[8] Given that these unreacted monomers have the potential to leach into nearby aqueous environments and enter the body, they may pose risks of toxicity.[9] Incomplete polymerization not only has the potential to result in the removal of monomers from the formed polymer but can also contribute to the natural degradation of the matrix. The degradation of the resin phase in composites within the oral environment may take place through processes like hydrolysis and aging, which can lead to the release of monomers as a result of the breakdown of the organic matrix.[9,10] Resin composite biodegradation may be linked to allergic reactions, bone loss or irritation of the oral mucosa.[12] The physicochemical characteristics of dental materials, particularly concerning the molecular size of monomers, their chemical compositions and the presence of various functional groups, are the primary factors contributing to biodegradation and the subsequent leaching of materials.[13,14] In the realm of dental materials research, biocompatibility investigations tied to quality control hold immense significance. To achieve this goal, cytotoxicity testing, which assesses cellular responses and the potential for cell death in response to new material formulations, plays a vital role in the development of novel dental materials. Minimizing and preventing cytotoxic effects are paramount, particularly in specialized fields such as endodontics and operative dentistry.[15]

One of the primary challenges with studies on cytotoxic effects is that they require a substantial amount of labor and time.[16] To streamline and enhance the screening of novel molecules in the development of materials, a practical solution is the adoption of in silico-based modeling approaches, such as quantitative structure–activity relationships (QSAR).[17] In contemporary QSAR studies, models are constructed by utilizing a variety of molecular descriptors derived from a specific molecule's structure. These descriptors have their own advantages and

limitations. Subsequently, they are transformed into a mathematical equation that correlates the biological activities of the examined molecules with their chemical attributes (molecular descriptors).[18,19] The development of a QSAR model necessitates not only a strong predictive capacity, robustness and goodness of fit but also a well-defined domain of applicability. Additionally, QSAR modeling is subject to regulation by the Organization for Economic Co-Operation and Development (OECD), which has established several criteria that must be met for a QSAR model to be deemed valid. One of the key criteria involves the mechanistic interpretation of molecular descriptors, which pertains to the utilization of descriptors linked to molecular structure and relevant molecular fragments.

In recent years, a Monte Carlo optimization method, where the analyzed activity is regarded as a random event, has gained prominence as a promising approach in QSAR modeling. This approach relies on a conformation-independent methodology and employs optimal descriptors derived from topological molecular characteristics, as well as molecules represented in the simplified molecular input line entry system (SMILES) notation.[20,21] The described method offers a significant advantage over more commonly used approaches due to its simplicity and efficiency. Additionally, this method can identify molecular fragments (calculated as SMILES notation descriptors) that influence the studied activity and can be linked to the chemical structures of the compounds under investigation The primary objective of this research is to create a conformation-independent QSAR model utilizing the Monte Carlo optimization method for predicting the cytotoxic effects of acrylic acid-based monomers. Furthermore, another key goal of this research was to identify SMILES notation descriptors linked to molecular fragments that exert both positive and negative impacts on cytotoxic effects.

EXPERIMENTAL

To initiate the development of suitable QSAR models, a total of 39 acrylic acid-based dental monomers were initially drawn using ACD/ChemSketch software version 11.0. These molecules were subsequently transformed into SMILES notation using the same software.[22] The chemical structures of the compounds utilized for QSAR modeling, along with their corresponding SMILES notations, can be found in Table S-I (Supporting material to this paper). In this QSAR modeling, the pertinent cytotoxic effect activity was assessed using pIC_{50} values against Hela S3 cell lines, data from the literature were converted to pIC_{50} values, calculated as $pIC_{50} = -\log IC_{50}$. Once we completed the construction of the relevant database, we proceeded to perform three distinct random divisions of the main molecule database into two sets: the training set, comprising 29 compounds (75 %), and the test set, comprising 10 compounds (25 %). We also assessed the normality of the activity distribution, following the method outlined in the published literature.[23]

To create conformation-independent QSAR models, we utilized the CORAL software (correlation and Logic, http://www.insilico.eu/coral), which is founded on the Monte Carlo method and its algorithm, considering the relevant activity as a random occurrence. We con-

sidered two categories of molecular descriptors derived from the molecular graph and SMILES notation. Concerning molecular graphs, we defined invariants as local graph invariants, including the Morgan extended connectivity index of increasing order (EC0), path numbers of lengths 2 and 3 (p2, p3), valence shells of ranges 2 and 3 (s2, s3), and the code of nearest neighbors (NNCk). In recent years, the SMILES notation has gained prominence as one of the most convenient representations, particularly in the field of chemoinformatics. SMILES notation is regarded as an appealing alternative to the traditional molecular graph representation. This characteristic is of great significance in medicinal chemistry because establishing correlations between molecular fragments and molecular graph-based descriptors can be quite complex.

The local SMILES attribute, entitled the "SMILES atom", is a SMILES string fragment with one ('C', 'N', '=') or two ('Cl', 'Br', '@@') symbols which cannot be decomposed further for conducting individual analyses. The calculation of DCW, one of the simplest local molecular descriptors, is performed with a mathematical function of the mentioned SMILES atoms. In essence, the approach translates every character found in the SMILES string into a numerical descriptor. To cite an example, the propionic acid molecule represented by the SMILES notation as "CCC(=O)O" can be considered. In this specific case, the calculation of the DCW could be performed on the basis of the individual CW characters:

$$DCW(\text{"CCC(=O)O"} = CW(\text{"C"}) + CW(\text{"C"}) + + CW(\text{"C"}) + CW(\text{"("}) + \\ + CW(\text{"="}) + CW(\text{"O"}) + CW(\text{")"}) + CW(\text{"O"}) \tag{1}$$

While valuable information is obtained from single atom-based local SMILES descriptors, in order to reveal more complex local chemical environments, one needs to go beyond individual atoms. Molecular fragments which significantly contribute to the overall molecular properties may be defined by combining two or three consecutive SMILES atoms. *DCW*s can then be calculated by using such fragments, further enhancing the information content available for QSAR modeling. For instance, propionic acid represented by the SMILES notation as "CCC(=O)O" could be considered. Through the combination of consecutive SMILES atoms, the following molecular fragments can be defined:

$$DCW(\text{"CCC(=O)O"}) = CW(\text{"CC"}) + CW(\text{"CC"}) + CW(\text{"C("}) + \\ + CW(\text{"("}) + CW(\text{"=O"}) + CW(\text{"O)"}) + CW(\text{")O"}) \tag{2}$$

When consecutive SMILES atoms are combined in order to define molecular fragments, there are significant advantages, although it is crucial to make certain considerations. For example, fragments such as "CO" and "OC" (or "CCO" and "OCC") are to be treated as distinct entities, which might lead to unreliable QSAR models and inaccurate representations. A normalized combination of SMILES atoms is applied in order to address this particular issue. The utilization of this approach ensures that the fragments are identified and consistently encoded irrespective of the order in which the atoms occur. In order to achieve this, specific algorithms need to be used, or it could be achieved by administering the SMILES notation canonization, which defines a unique order on the basis of the atomic symbols.[20,21] Global SMILES attribute based descriptors encompass broader characteristics of the whole molecule, such as whether specific functional groups or atom combinations are present or absent.[20,21] The information available for QSAR modeling can significantly be enriched through the incorporation of both local and global SMILES-based descriptors. What is more, SMILES notation-based molecular descriptors present a mechanistic interpretation, considering that this particular feature is in correlation with molecular fragments.[20,21] The numerical value of every SMILES notation descriptor that a molecule has contributes to the correlation weight of the

said molecule (DCW), which is defined as the sum of all the defined correlation weights (CW) of SMILES descriptors:

$$DCW(T,N_{epoch}) = zCW(\text{ATOMPAIR}) + xCW(\text{NOSP}) + yCW(\text{BOND}) + tCW(\text{HALO}) + \\ + rCW(\text{HARD}) + \alpha\Sigma CW(S_k) + \beta\Sigma CW(SS_k) + \gamma\Sigma CW(SSS_k) \qquad (3)$$

where z, x, y, t, α, β and γ are numbers 1 (yes) or 0 (no), while their values determine whether the specific SMILES descriptor is used in the development of the model. Symbol S_k represents one SMILES notation symbol (or two that are inseparable), and is related to the local descriptors. These local descriptors also represent linear combinations of two or three SMILES atoms, represented by symbols SS_k and SSS_k, respectively. This study includes the following global SMILES notation-based descriptors: HALO, ATOMPAIR, BOND, HARD and NOSP, all defined in accordance with the published methodology.[20,21] The molecules' DCW was calculated by using Eq. (4) because the QSAR model development in this study was performed by combining both the SMILES notation (global and local) and the local graph invariant descriptors, considering that this hybrid molecular descriptor approach ensures the development of more accurate and robust QSAR models than the ones based on a single type of descriptor:

$$DCW(T,N_{epoch}) = \Sigma CW(S_k) + \Sigma CW(SS_k) + \Sigma CW(SSS_k) + \Sigma CW(\text{EC0}_k) + \Sigma CW(\text{PT2}_k) + \\ + \Sigma CW(\text{PT3}_k) + \Sigma CW(\text{VS2}_k) + \Sigma CW(\text{VS3}_k) + \Sigma CW(\text{NNC}_k) \qquad (4)$$

In addition to the aforementioned symbols: S_k, SS_k and SSS_k, Eq. (2) uses the following symbols as well: the Morgan connectivity index of the zero order (with the hydrogen suppressed graph) – EC0_k, paths in the lengths of 2 and 3 – PT2_k and PT3_k; valence shells 2 and 3 – VS2_k and VS3_k; nearest neighbors – NNC_k. The calculation of all the above-defined molecular descriptors was made with the CORAL software (http://www.insilico.eu/coral). In this study, we employed all SMILES notation-based descriptors, encompassing local, global and HARD-index descriptors. A notable characteristic of the resulting QSAR model, developed using the Monte Carlo method, is the calculation of correlation weight (CW), which assigns a numerical value to each of the optimal descriptors utilized.[21] The methodology for accomplishing this process involves the generation of appropriate random numbers and assessing the fraction of numbers that conform to certain properties. In this process, CW values are randomly allocated to all employed optimal descriptors, encompassing both molecular graph-based and SMILES notation-based descriptors, in each individual Monte Carlo run. The Monte Carlo optimization procedure is then extended to compute the numerical data for the correlation weights, which aim to maximize the correlation coefficient between the studied activity and the employed optimal descriptors. In this context, the Monte Carlo method relies on two parameters: threshold (T) and the number of epochs (N_{epoch}).

In the creation of QSAR models, we explored values ranging from 0 to 10 for T and from 0 to 70 for Nepoch. The process of identifying the most predictive combination of T and N_{epoch} was determined based on a methodology outlined in published references.[24-26] The primary objective of any QSAR modeling process is to create a robust model that can predict the properties of new molecules with objectivity, reliability, and precision. To assess the quality of the developed QSAR models, we employed the following methods: internal validation using the training set, external validation using the validation set and data randomization through a Y-scrambling test. We accomplished this by employing various statistical parameters, including the correlation coefficient (r^2), cross-validated correlation coefficient (q^2), standard error of estimation (s), mean absolute error (MAE), Fischer ratio (F), root-mean-square error ($RMSE$), R_m^2, and MAE-based metrics.[23,27-31] Recently, a novel criterion known

as the index of ideality of correlation (*IIC*) has been proposed for evaluating the predictive capacity of QSAR models.[25,26] This criterion takes into account not only the correlation coefficient but also the distribution of data points relative to the diagonal line, in the coordinates of observed and calculated values for the studied endpoint. The set of correlation weights: $CW(x)$ are coefficients producing a maximal value of the target function within the Monte Carlo optimization procedure and the target function can be defined as:

$$TF = R_{\text{training}} + R_{\text{invisible-training}} - \left| R_{\text{training}} - R_{\text{invisible-training}} \right| \times \text{Const.} \tag{5}$$

where R_{training} is the correlation coefficient between endpoint and the $DCW(T^*, N^*)$ for compounds in the training set, the $R_{\text{invisible-training}}$ corresponds to the same parameter in the invisible training set; praxis has shown that Const. = 0.1 is a more or less satisfactory choice for manifold computational experiments with different endpoints. However, while keeping the value of Const. invariant, the target function can be modified as:

$$TF_{\text{m}} = TF + IIC \times \text{Const.} \tag{6}$$

with the IIC parameter calculated as the following form:

$$IIC_{\text{test}} = r_{\text{test}} \times \frac{\min(^-MAE_{\text{test}}, {}^+MAE_{\text{test}})}{\max(^-MAE_{\text{test}}, {}^+MAE_{\text{test}})} \tag{7}$$

where, using the differences:

$$\Delta_k = \text{Observed}_k - \text{Calculated}_k \tag{8}$$

With data available for all Δ_k values in the test set, it is possible to compute the sum of negative and positive Δ_k values, akin to the calculation of mean absolute error (*MAE*):

$$^-MAE_{\text{test}} = \frac{1}{-N} \sum_{k=1}^{-N} \left| \Delta_k \right|, \quad \Delta_k < 0, \ {}^-N \text{ is the number of } \Delta_k < 0 \tag{9}$$

$$^+MAE_{\text{test}} = \frac{1}{+N} \sum_{k=1}^{+N} \left| \Delta_k \right|, \quad \Delta_k \geq 0, \ {}^-N \text{ is the number of } \Delta_k \geq 0 \tag{10}$$

RESULTS AND DISCUSSION

The concept of the applicability domain (*AD*) plays a pivotal role in guiding the selection of molecules.[32–34] To establish the *AD*, we followed a published methodology and confirmed that all molecules in this study fell within the defined *AD* range, with no outliers identified.[21] Utilizing the least squares method, we present the most optimal QSAR models for the studied activity, with respect to the T and N_{epoch} values, in the form:

Split 1: $pIC_{50} = -0.3378(\pm0.0938) + 0.0194(\pm0.0005) \times DCW(4,9)$ (11)

Split 2: $pIC_{50} = 0.2293(\pm0.0350) + 0.0411(\pm0.0005) \times DCW(1,6)$ (12)

Split 3: $pIC_{50} = 0.3749(\pm0.0353) + 0.0326(\pm0.0005) \times DCW(1,18)$ (13)

The values of the statistical metrics used to assess the quality of the developed QSAR models for predicting the cytotoxicity of acrylic acid-based dental monomers are presented in Table S-I. These metrics suggest that the method employed was successful in creating a QSAR model with good reproducibility, which was further validated using the concordance correlation coefficient. The

predictability of the developed QSAR model was assessed based on the values presented in Table S-II of the Supplementary material, confirming the model's validity. Additionally, the model was classified as valid using *MAE*-based metrics. We conducted the ultimate evaluation of the developed QSAR models, both for the training and the test set, using the index of ideality of correlation and obtained values that indicate the high predictive potential of the developed QSAR models. Furthermore, we conducted *Y*-randomization, involving the random shuffling of *Y* values in 1000 trials across ten separate runs, to gauge the robustness of the developed QSAR models.[23] The values shown in Table S-III of the Supplementary material suggest that there was no chance correlation among the developed models. Among the statistical methods used, the most favorable QSAR model was derived from the first split. Notably, the best model was achieved with a *T* value of 4, and the most suitable N_{epoch} value was determined to be 9. The most successful Monte Carlo optimization runs (with the highest r^2 values) for the developed QSAR models from all splits are visually depicted in Figs. 1–3.
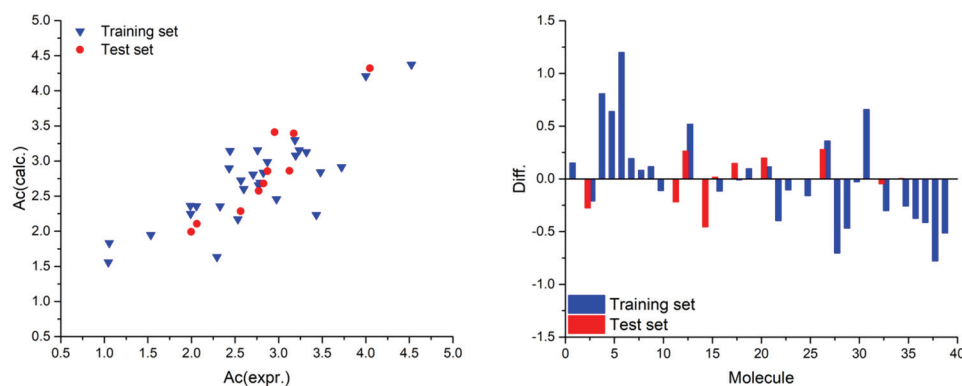

Fig. 1. Graphical presentation of the best Monte Carlo optimization run (the highest value for r^2) for the developed QSAR model for Split 1. (*Ac*(expr.) – experimental value for molecule p*IC*$_{50}$; *Ac*(calc.) – calculated value for molecule p*IC*$_{50}$ using developed QSAR model; Diff. = *Ac*(expr.) – *Ac*(calc.).

One of the primary objectives of this study was to identify molecular fragments, characterized as the SMILES notation's optimal descriptors, that exert both positive and negative effects on the studied activity.[21,35–37] The complete list of molecular descriptors, which are derived from both the SMILES notation and the molecular graph, can be found in Table S-IV of the Supplementary material. An illustration of the calculation of a molecule's summarized correlation weight (*DCW*) and the studied activity (p*IC*$_{50}$) is provided in Table I. In this example, molecular graph-based descriptors were excluded to facilitate a more straightforward interpretation.
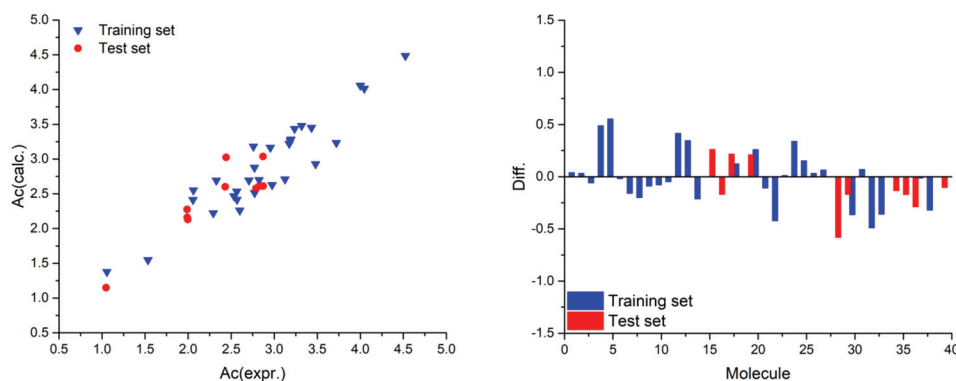
Fig. 2. Graphical presentation of the best Monte Carlo optimization run (the highest value for r^2) for the developed QSAR model for Split 2. (Ac(expr.) – experimental value for molecule pIC_{50}; Ac(calc.) – calculated value for molecule pIC_{50} using developed QSAR model; Diff. = Ac(expr.) – Ac(calc.).
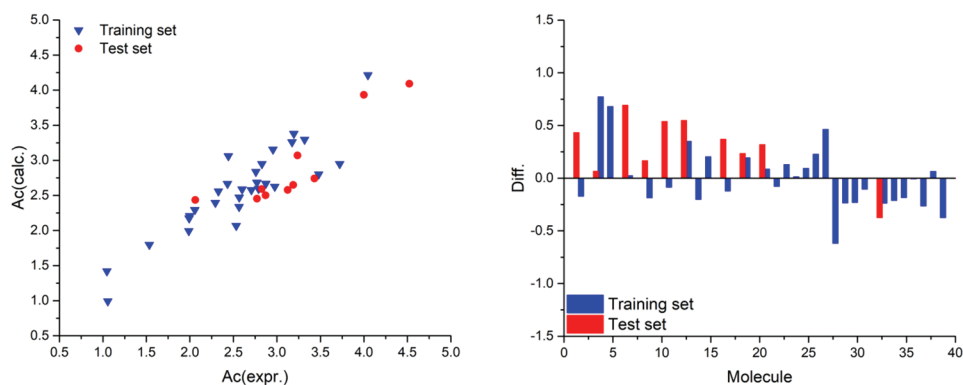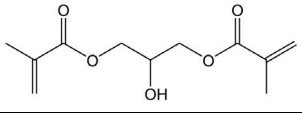

Fig. 3. Graphical presentation of the best Monte Carlo optimization run (the highest value for r^2) for the developed QSAR model for Split 3. (Ac(expr.) – experimental value for molecule pIC_{50}; Ac(calc.) – calculated value for molecule pIC_{50} using developed QSAR model; Diff. = Ac(expr.) – Ac(calc.).

Following the published methodology, we categorized the obtained SA_ks as promoters of the cytotoxicity of acrylic acid-based dental monomers.[21,35–37] In Table II, we have listed selected SAKs along with their mechanistic interpretations, while the complete list can be found in Table S-II. We have provided an analysis of the contribution of molecular fragments to the cytotoxicity of acrylic acid-based dental monomers in Fig. 4. In the presented figure, green denotes groups that have a positive influence, while red denotes groups that have a negative influence on the studied effect. As mentioned, each SA_K contributes its CW value.

TABLE I. Example of DCW calculation

	IUPAC name: [2-hydroxy-3-(2-methylprop-2-enoyloxy)propyl]--2-methylprop-2-enoate
	SMILES notation: OC(COC(=O)C(=C)C)COC(=O)C(=C)C $DCW = 57.88841$ pIC_{50}(calc.) = 2.6094

SA_k	$CW(SA_k)$	SA_k	$CW(SA_k)$	SA_k	$CW(SA_k)$	SA_k	$CW(SA_k)$
1000100000	2.0407	BOND10000	1.411	Cmax.0......	0.0745	O...=.......	–0.9669
(..........	2.3831	C...(.......	–0.8598	HALO00000	3.1001	O...C...(...	1.0934
(...C...(...	–0.5923	C...(...=...	–0.916	Nmax.0......	1.8318	O...C.......	–0.922
++O---B2=	2.9389	C...(...C...	1.4187	NOSP01000	1.9941	Omax.5......	0
=...(.......	–0.7396	C...........	–0.8583	O...(.......	–0.6732	Smax.0......	2.3577
=..........	–0.0911	C...=...(...	–0.9573	O...(...C...	2.1158	O...=...(...	–0.5599
=...C...(...	2.1233	C...=.......	4.2232	O...........	–0.5305		
=...O...(...	–0.4744	C...O...C...	–0.6593				

TABLE II. Mechanistic interpretation of selected SA_ks

Promoters of pIC_{50} increase		Promoters of pIC_{50} decrease	
(...(....... (..........	Simple molecular branching and complex	(...O...(...	Complex molecular branching with oxygen atom involving
		++++N--- B2==	Presence of independent nitrogen atom and double bond in molecule
C...(....... (...C...(...	Molecular branching on carbon atom	++++N--- O===	Presence of independent nitrogen and oxygen atoms in molecule
		=..........	Double bond
++++O--- B2==	Presence of independent oxygen atom and double bond in molecule	=...(.......	Double bond involved in molecular branching
1..........	Presence of ring in molecule	=...O...(...	Double bond with oxygen atom involved in molecular branching
C...1....... C...1...C...	Presence of ring in molecule with carbon atoms	C...(...=...	Double bond with carbon atom involved in molecular branching
N...C...C...	Ethyl amine fragment	C..........	Carbon atom
C...=....... C...=...C...	Double bond with carbon atom	N..........	Nitrogen atom
		O..........	Oxygen atom
C...N...C...	Sequence of carbon-nitrogen-carbon atoms	N...C.......	Methyl amine group, or sequence of nitrogen-carbon atom
c.......... c...c.......	Aromatic carbon in molecular structure	c...(...C...	Branched carbon atom bounded to aromatic carbon
c...C....... c...O.......	Carbon or oxygen atom bounded to aromatic carbon	c...O...C...	Methyl group bounded to aromatic carbon

Based on the results obtained from QSAR modeling, the SMILES notation descriptors associated with molecular fragments that have a positive impact on pIC_{50} for the cytotoxicity of acrylic acid-based dental monomers, leading to a decrease in cytotoxicity, include: "C...C..." (ethyl group) – representing two carbon atoms in sequence in any part of the molecule; "O...C..." (methoxy group) –

denoting a sequence of oxygen and carbon atoms in any part of the molecule; "O...C...C" (ethoxy group) – representing oxygen and two carbon atoms in sequence in any part of the molecule.
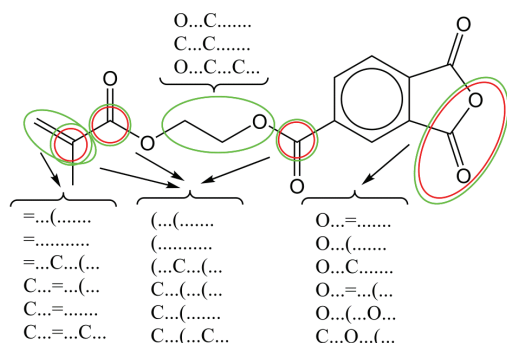

Fig. 4. Molecular fragments contribution to the cytotoxicity of acrylic acid-based dental monomers (green – increase, red – decrease).

In more complex molecular groups, some fragments contribute to an increase in the pIC_{50} value, while others contribute to a decrease. Therefore, to fully understand how these complex molecular fragments influence the cytotoxicity effect, it is essential not only to perform a qualitative analysis of individual molecular fragments but also a quantitative analysis of their *CW* numerical values. For instance, a molecular fragment found in Fig. 2 that incorporates a carboxyl group contains specific subfragments that either exert a detrimental influence on pIC_{50}, such as "C............" representing a solitary carbon atom or a methyl group, "O............" signifying an individual oxygen atom, "=..........." indicating the presence of a double bond, "=...(......." denoting a double bond integrated into molecular branching, and "C a double bond with a carbon atom involved in molecular branching." In contrast, within the same carboxyl group, there are subfragments with a beneficial effect on pIC_{50}, including "(...(......." and "(..........." – both linked to molecular branching, "C...(......." and "(...C...(..." – related to branching on carbon atoms and "C...=......" and "C...=...C..." – subfragments associated with double bonds featuring carbon atoms. This illustrates how intricate molecular structures can encompass various subfragments that contribute both positively and negatively to the observed cytotoxicity effect, underscoring the necessity for a comprehensive qualitative and quantitative analysis.

CONCLUSION

The primary objective of this research is to create robust QSAR models capable of predicting the cytotoxicity of acrylic acid-based dental monomers with high predictability. This predictability is assessed through the use of various statistical parameters. The conformation-independent models, developed based on optimal descriptors derived from both local graph and SMILES notation invariants, are calculated using the Monte Carlo optimization method. The application

of a variety of statistical techniques allowed for the assessment of the predictive potential and robustness of the developed QSAR models. The validity of these models is confirmed by the numerical values obtained during their validation. The Monte Carlo optimization method effectively identified molecular fragments, which are employed as SMILES notation fragments in QSAR modeling, with both positive and negative effects on the cytotoxicity of acrylic acid-based dental monomers. In conclusion, the methodology presented in this research can be employed to pursue the development of new dental materials with reduced cytotoxicity.

SUPPLEMENTARY MATERIAL

Additional data and information are available electronically at the pages of journal website: https://www.shd-pub.org.rs/index.php/JSCS/article/view/12828, or from the corresponding author on request.

ИЗВОД

QSAR МОДЕЛОВАЊЕ ЦИТОТОКСИЧНОСТИ ДЕНТАЛНИХ МОНОМЕРА БАЗИРАНИХ НА ДЕРИВАТИМА АКРИЛНЕ КИСЕЛИНЕ ПРИМЕНОМ МОНТЕ КАРЛО ОПТИМИЗАЦИЈЕ

МИРЈАНА БОШКОВИЋ[1], САША СТАНКОВИЋ[1], ЈЕЛЕНА В. ЖИВКОВИЋ[2] и АЛЕКСАНДАР М. ВЕСЕЛИНОВИЋ[2*]

[1]Универзитет у Нишу, Медицински факултет, Катедра Стоматолошка протетика, Булевар др Зорана Ђинђића 81, Ниш и [2]Универзитет у Нишу, Медицински факултет, Катедра Хемија, Булевар др Зорана Ђинђића 81, Ниш

Полимери који се примењују у стоматолошкој пракси често су формирани помоћу деривата акрилне киселине као почетног мономера. Међутим, наведени деривати показују цитотоксичност према различитим типовима ћелија, што је ефекат који мора бити смањен у будућим материјалима. Основни циљ овог истраживања је да се успостави QSAR модел за предвиђање цитотоксичних ефеката деривата акрилне киселине као и да идентификује молекулске фрагменте, молекулске дескрипторе са механичким тумачењем, који имају утицај на цитотоксичност. Основни алгоритам за добијање QSAR модела био је Монте Карло техника оптимизације, а модели су користили конформационо независне молекулске дескрипторе засноване на молекуларном графу и на SMILES нотацији. Различити статистички параметри су коришћени да би се валидирали добијени QSAR модели и добијени резултати указују на добру предиктивност QSAR модела. С обзиром на то да већина база података молекула користи SMILES нотацију за представљање молекулске структуре, представљени QSAR модели могу послужити као брз и ефикасан алат за претрагу нових мономера.

(Примљено 1. марта, ревидирано 15. априла, прихваћено 2. јуна 2024)

REFERENCES

1. I. M. Barszczewska-Rybarek, *Materials (Basel)* **12** (2019) 4057 (https://doi.org/10.3390/ma12244057)
2. N. Moszner, T. Hirt, *J. Polym. Sci. Pol. Chem.* **50** (2012) 4369 (https://doi.org/10.1002/pola.26260)
3. D. Dressano, M. V. Salvador, M. T. Oliveira, G. M. Marchi, B. M. Fronza, M. Hadis, W. M. Palin, A. F. Lima, J. Mech, *Behav. Biomed. Mater*. **110** (2020) 103875 (https://doi.org/10.1016/j.jmbbm.2020.103875)
4. R. Gautam, R. D. Singh, V. P. Sharma, R. Siddhartha, P. Chand, R. Kumar, *J. Biomed. Mater. Res., B* **100** (2012) 1444 (https://doi.org/10.1002/jbm.b.32673)
5. E. C. Kim, H. Park, S. I. Lee, S. Y. Kim, *Basic Clin. Pharm.* **117** (2015) 340 (https://doi.org/10.1111/bcpt.12404)
6. M. Goldberg, *Clin. Oral Investig.* **12** (2008) 1 (https://doi.org/10.1007/s00784-007-0162-8)
7. S. K. Jun, J. R. Cha, J. C. Knowles, H. W. Kim, J. H. Lee, H. H. Lee, *Dent. Mater.* **36** (2020) 157 (https://doi.org/10.1016/j.dental.2019.11.016)
8. J. G. Leprince, W. M. Palin, M. A. Hadis, J. Devaux, G. Leloup, *Dent. Mater.* **29** (2013) 139 (https://doi.org/10.1016/j.dental.2012.11.005)
9. T. Hampe, A. Wiessner, H. Frauendorf, M. Alhussein, P. Karlovsky, R. Bürgers, S. Krohn, *Polymers (Basel)* **14** (2022) 1790 (https://doi.org/10.3390/polym14091790)
10. L. S. Mokeem, I. M. Garcia, M. A. Melo, *Biomedicines* **11** (2023) 1256 (https://doi.org/10.3390/biomedicines11051256)
11. F. Amin, M. A. Fareed, M. S. Zafar, Z. Khurshid, P. J. Palma, N. Kumar, *Coatings* **12** (2022) 1094 (https://doi.org/10.3390/coatings12081094)
12. S. Bandarra, P. Mascarenhas, A. R. Luis, M. Catrau, E. Bekman, A. C. Ribeiro, S. Félix, J. Caldeira, I. Barahona, *Clin. Oral Investig.* **24** (2020) 2691 (https://doi.org/10.1007/s00784-019-03131-4)
13. A. Bakopoulou, T. Papadopoulos, P. Garefis, *Int. J. Mol. Sci.* **10** (2009) 3861 (https://doi.org/10.3390/ijms10093861)
14. M. Cadenaro, T. Maravic, A. Comba, A. Mazzoni, L. Fanfoni, T. Hilton, J. Ferracane, L. Breschi, *Dent. Mater.* **35** (2019) e1 (https://doi.org/10.1016/j.dental.2018.11.012)
15. G. Cervino, M. Cicciù, A. S. Herford, A. Germanà, L. Fiorillo, *Materials (Basel)* **13** (2020) 3350 (https://doi.org/10.3390/ma13153350)
16. I. P. Caldas, G. G. Alves, I. B. Barbosa, P. Scelza, F. de Noronha, M. Z. Scelza, *Dent. Mater.* **35** (2019) 195 (https://doi.org/10.1016/j.dental.2018.11.028)
17. E. N. Muratov, J. Bajorath, R. P. Sheridan, I. V. Tetko, D. Filimonov, V. Poroikov, T. I. Oprea, I. I. Baskin, A. Varnek, A. Roitberg, O. Isayev, S. Curtarolo, D. Fourches, Y. Cohen, A. Aspuru-Guzik, D. A. Winkler, D. Agrafiotis, A. Cherkasov, A.Tropsha, *Chem. Soc. Rev.* **49** (2020) 3525 (https://doi.org/10.1039/d0cs90041a)
18. P. Liu, W. Long, *Int. J. Mol. Sci.* **10** (2009) 1978 (https://doi.org/10.3390/ijms10051978)
19. N. Tripathi, M. K. Goshisht, S. K. Sahu, C. Arora, *Mol. Divers.* **25** (2021) 1643 (https://doi.org/10.1007/s11030-021-10237-z)
20. A. P. Toropova, A. A. Toropov, *Mini Rev. Med. Chem.* **18** (2018) 382 (https://doi.org/10.2174/1389557517666170927154931)
21. A. M. Veselinović, J. B. Veselinović, J. V. Živković, G. M. Nikolić, *Curr. Top. Med. Chem.* **15** (2015) 1768 (https://doi.org/10.2174/1568026615666150506151533)
22. A. K. Halder, A. H. S. Delgado, M. N. D. S. Cordeiro, *Dent. Mater.* **38** (2022) 333 (https://doi.org/10.1016/j.dental.2021.12.014)

23. P. K. Ojha, K. Roy, *Chemometr. Intell. Lab.* **109** (2011) 146 (https://doi.org/10.1016/j.chemolab.2011.08.007)
24. V. Stoičkov, D. Stojanović, I. Tasić, S. Šarić, D. Radenković, P. Babović, D. Sokolović, A. M. Veselinović, *Struct. Chem.* **29** (2018) 441 (https://doi.org/10.1007/s11224-017-1041-9)
25. A. A. Toropov, A. P. Toropova, *Mutat. Res.-Gen. Tox. En.* **819** (2017) 31 (https://doi.org/10.1016/j.mrgentox.2017.05.008)
26. A. M. Veselinović, A. Toropov, A. Toropova, D. Stanković-Đorđević, J. B. Veselinović, *New J. Chem.* **42** (2018) 10976 (https://doi.org/10.1039/C8NJ01034J)
27. P. K. Ojha, K. Roy, *Chemometr. Intell. Lab. Syst.* **109** (2011) 146 (https://doi.org/10.1016/j.chemolab.2011.08.007)
28. P. K. Ojha, I. Mitra, R. N. Das, K. Roy, *Chemometr. Intell. Lab. Syst.* **107** (2011) 194 (https://doi.org/10.1016/j.chemolab.2011.03.011)
29. P. P. Roy, J. T. Leonard, K. Roy, *Chemometr. Intell. Lab. Syst.* **90** (2008) 31 (https://doi.org/10.1016/j.chemolab.2007.07.004)
30. K. Roy, R. N. Das, P. Ambure, R. B. Aher. *Chemometr. Intell. Lab.* **152** (2016) 18 (https://doi.org/10.1016/j.chemolab.2016.01.008)
31. L. I. Lin, *Biometrics* **45** (1989) 255 (https://doi.org/10.2307/2532051)
32. O. Nicolotti, D. Gadaleta, G. F. Mangiatordi, M. Catto, A. Carotti, *IJQSPR* **1** (2016) 45 (https://doi.org/10.4018/IJQSPR.2016010102)
33. P. Gramatica, *QSAR Comb. Sci.* **26** (2007) 694 (https://doi.org/10.1002/qsar.200610151)
34. P. Gramatica, A. Sangion, *J. Chem. Inf. Model.* **56** (2016) 1127 (https://doi.org/10.1021/acs.jcim.6b00088)
35. M. Zivkovic, M. Zlatanovic, N. Zlatanovic, M. Golubović, A. M. Veselinović, *Mini Rev. Med. Chem.* **20** (2020) 1389 (https://doi.org/10.2174/1389557520666200212111428)
36. S. A. Amin, N. Adhikari, S. Gayen, T. Jha, *J. Biomol. Struct. Dyn.* **37** (2019) 4528 (https://doi.org/10.1080/07391102.2018.1552895)
37. S. Ahmadi, S. Lotfi, S. Afshari, P. Kumar, E. Ghasemi, *SAR QSAR Environ. Res.* **32** (2021) 1013 (https://doi.org/10.1080/1062936X.2021.2003429).